Supplemental Information

$G_s\alpha$ deficiency in the dorsomedial hypothalamus underlies obesity associated with $G_s\alpha$ mutations

Min Chen[1*], Yogendra B. Shrestha[1*], Brandon Podyma[1,3], Zhenzhong Cui[2], Benedetta Naglieri[1], Hui Sun[1], Thuy Ho[1,3], Eric A. Wilson[1], Yong-Qi Li[1], Oksana Gavrilova[2], and Lee S. Weinstein[1]

[1]Metabolic Diseases Branch and [2]Mouse Metabolism Core Laboratory, National Institute of Diabetes, Digestive, and Kidney Diseases, National Institutes of Health, Bethesda, Maryland, USA

[3]Present address: University of Virginia School of Medicine, Virginia, USA

[*]Co-first author

Supplemental Methods

Chronic cold adaptation. For chronic cold adaptation, mice were kept in individual cages with bedding within a climate control chamber (Memmert 750 LIFE Chamber) and kept in 30°C for 3 d to minimize SNS activity, and temperature was lowered to 22°C and then decreased by 2°C/d until 6°C was reached. At that point the mice were housed at 6°C for a further 7 d. Mice had full access to food and water throughout and showed no obvious untoward effects during adaptation.

Immunohistochemistry. Fat pads were fixed with 10% formalin. Tissue sections (5-μm thick for BAT and 8-μm thick for WAT) were treated in 10 mM sodium citrate, 0.05% Tween 20 at 85°C for 20 min, and then in 3% hydrogen peroxide for 10 min. After blocking in 5% BSA for 20 min, the sections were incubated with anti-F4/80 antibody (Biorad, catalog #MCA497; 1:100 dilution) or anti-UCP1 antibody (Abcam, catalog #Ab10983; 1:1000 dilution) at 4°C overnight, and then incubated with biotinylated goat anti-rabbit IgG secondary antibody (Agilent DAKO, catalog #E043201-6; 1:500 dilution) at room temperature for 1 h. The F4/80 or UCP1 signals were detected using streptavidin-horse radish peroxidase (Vector Laboratories), and visualized with diaminobenzidine tetrahydrochloride (Sigma). The sections were counterstained with hematoxylin.

Immunoblotting. BAT samples were homogenized in 1 x RIPA buffer (Cell Signaling) supplemented with protease inhibitor cocktail tablet. Lysates were centrifuged at 13,000 rpm for 10 min at 4°C, and the supernatants were used for immunoblotting. Protein extracts (30 μg) were separated on NovexN uPAGE 4-12% Bis-Tris gels (Life Technologies) and transferred using an iBlot 2 Dry Blotting System (Life Technologies), which was sequentially incubated with anti-UCP1 (Abcam, catalog #Ab10983) and anti-

α-tubulin antibodies (Calbiochem, catalog #CP06). Bands were quantified using the ChemiDOC MP imaging system (Biorad) and UCP1 protein levels were normalized to α-tubulin protein levels.

Supplemental Figure 1

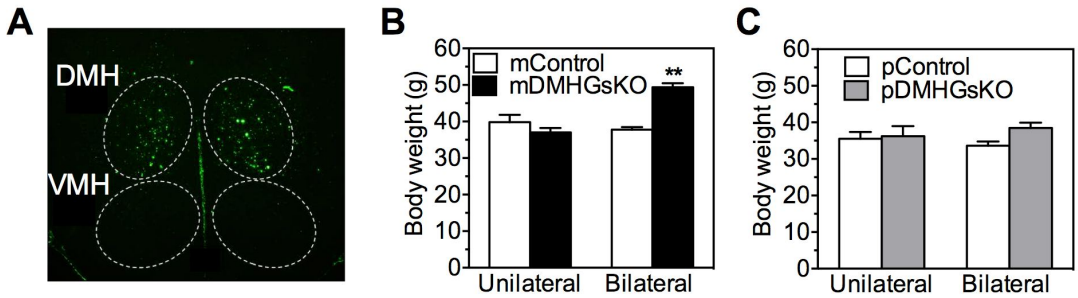

Supplemental Figure 1. Confirmation of stereotaxic injection position in DMHGsKO mice. (**A**) Representative image of AAV-Cre-GFP location indicated with green fluorescence. VMH, ventromedial nucleus of hypothalamus. (**B**) Body weight of mDMHGsKO and their control littermates at 4-5 mo post-injection separated by mice in which the injection into DMH was confirmed to be correctly targeted either unilaterally (n = 4-6/group) or bilaterally (n = 17-25/group). (**C**) Body weight of pDMHGsKO mice and their control littermates at 4-5 mo post-injection separated by mice in which the injection into DMH was confirmed to be correctly targeted either unilaterally (n = 2-4/group) or bilaterally (n = 5-10/group). Data are mean ± SEM. $^{**}P < 0.01$ vs. controls by Students *t* test.

Supplemental Figure 2

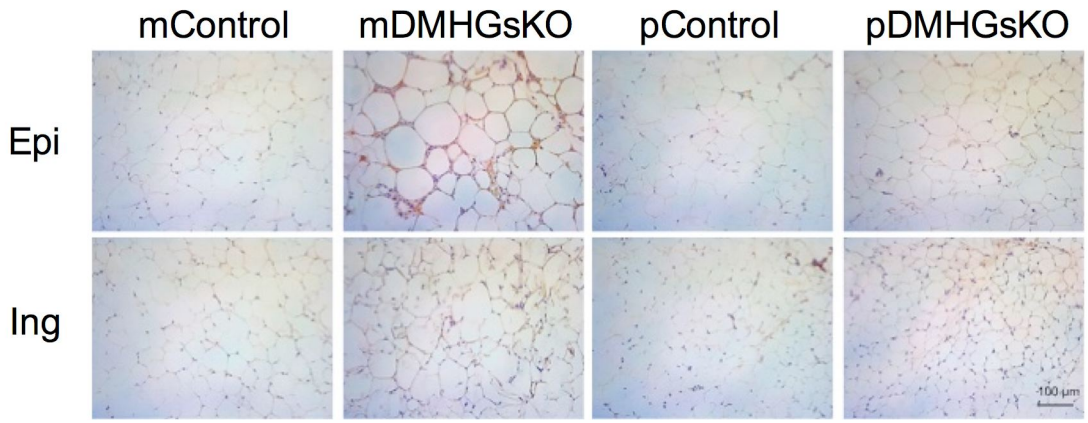

Supplemental Figure 2. Increased inflammation in mDMHGsKO white adipose tissue. Representative immunohistochemical staining for the macrophage marker F4/80 in epididymal (Epi) and inguinal (Ing) WAT from mDMHGsKO and pDMHGsKO mice and their respective controls (scale bar, 100 μM).

Supplemental Figure 3

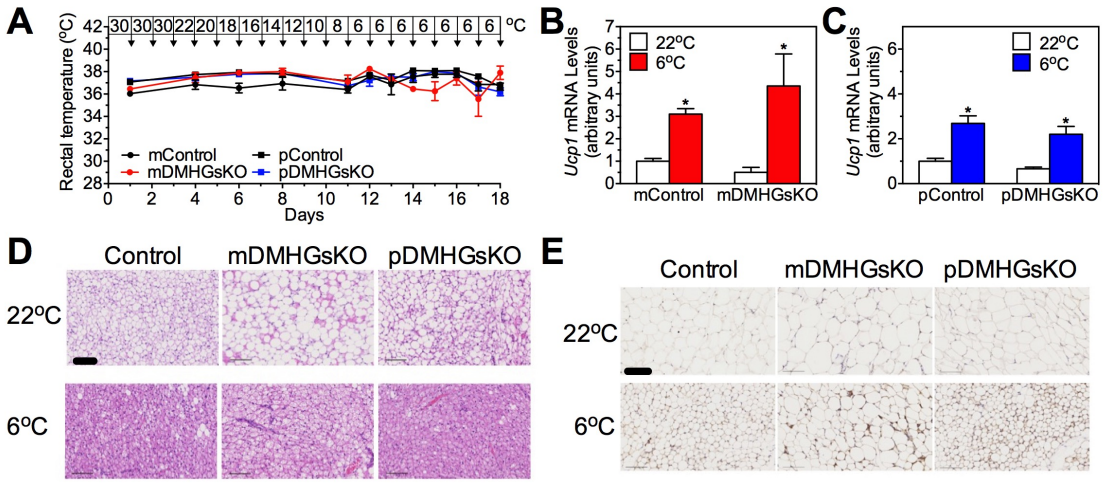

Supplemental Figure 3. WAT and BAT adaptation to chronic cold exposure. (**A**) Rectal temperature in mDMHGsKO and pDMHGsKO mice and their respective controls (n = 3/group) after exposure to gradually declining of ambient temperature down to 6°C and maintaining 6°C for 7 d (temperature during each day indicated on top of graph). (**B** and **C**) BAT *Ucp1* gene expression in (**B**) mDMHGsKO and (**C**) pDMHGsKO mice and their respective controls after being maintained at room temperature (22°C) or after chronic cold adaptation as outlined in panel A (n = 3/group). (**D**) H & E stained sections of BAT from control, mDMHGsKO, and pDMHGsKO mice either maintained at 22°C or after chronic cold adaptation to 6°C (scale bar, 100 μm) (**E**) Immunohistochemistry with an anti-UCP1 antibody of inguinal WAT sections from the same mice as panel D. The data in panels D and E is representative of what was observed in 3 mice per group. Data are mean ± SEM. $^{**}P < 0.05$ vs. 22°C by Students *t* test.

Supplemental Figure 4

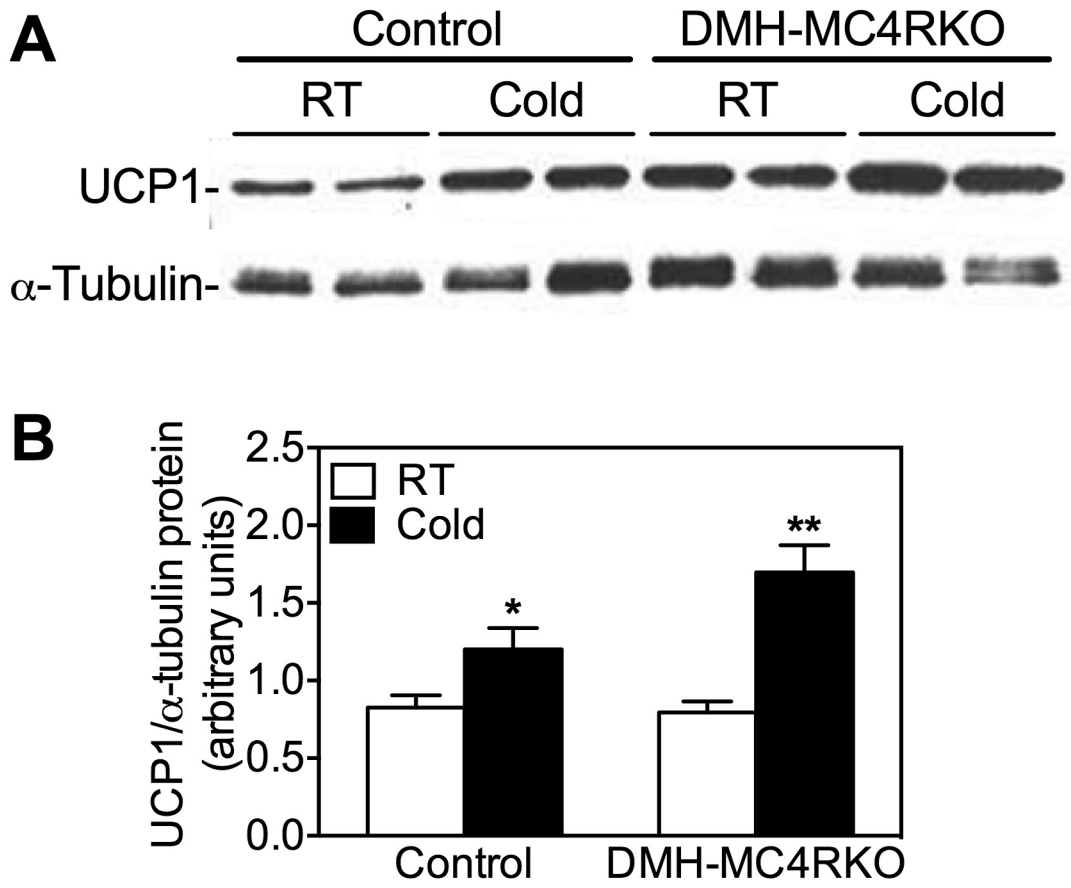

Supplemental Figure 4 BAT UCP1 protein response to cold in control and DMH-MC4RKO mice. (**A**) Representative immunoblot (one of two experiments) for BAT UCP1 and α-tubulin protein levels in male control and DMH-MC4RKO mice at room temperature (22°C, RT) and after 6 h at 4°C (Cold). (B) Quantitation of UCP1 protein levels normalized to α-tubulin (n = 4-5/group) Data are mean ± SEM. $^{*}P < 0.05$ or $^{**}P < 0.01$ vs. RT by Students *t* test.

Supplemental Figure 5

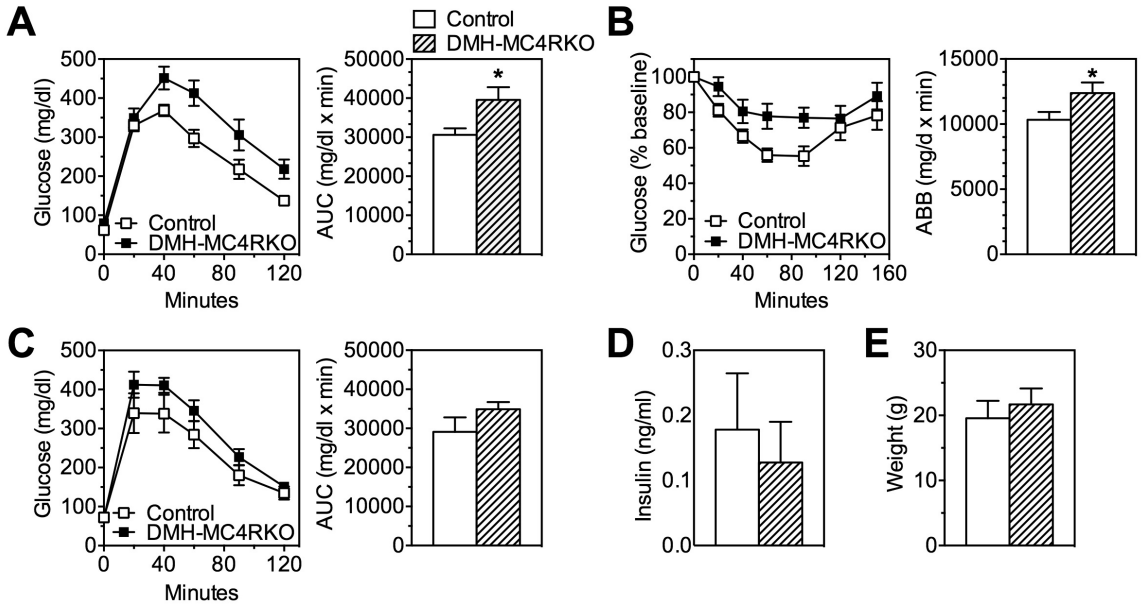

Supplemental Figure 5. Glucose metabolism in DMH-MC4RKO mice. (**A**) Glucose tolerance test (left panel) and areas under curve (AUC, right panel) performed on male DMH-MC4RKO and control mice at 2-2.5 mo post-injection (n = 11-13/group). (**B**) Insulin tolerance test (left panel) and areas below baseline (ABB, right panel) in the same mice (n = 11-14/group). (**C**) Glucose tolerance test (left panel) and areas under curve (AUC, right panel) performed on male DMH-MC4RKO and control mice at 2 wk post-injection (n = 5-7/group). (**D**) Fasting insulin levels in DMH-MC4RKO and control mice at 2 wk post-injection (n = 4-5/group). (**E**) Body weights of mice studied in panel C. Data are mean ± SEM. *$P < 0.05$ vs. control by Students *t* test.

Supplemental Figure 6

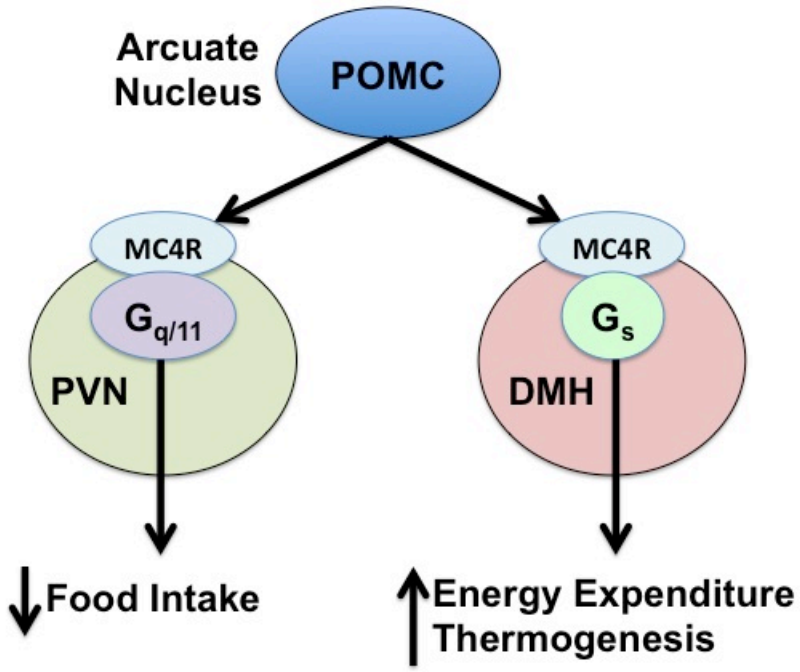

Supplemental Figure 6. Present model of G proteins involved in MC4R actions. POMC neurons from the arcuate nucleus project to the PVN and DMH, respectively. Activation of MC4R by release of melanocortins in PVN results in reduced food intake via activation of $G_{q/11}\alpha$, while activation of MC4R in DMH leads to increased energy expenditure and thermogenesis via activation of $G_s\alpha$.

Supplemental Table 1

Supplemental Table 1. Serum chemistries in fed DMH-MC4RKO and control mice at 2-2.5 mo post-injection

	DMH-MC4RKO	**Control**
Glucose (mg/dl)	156 ± 4	212 ± 25
Insulin (ng/ml)	3.9 ± 1.1	11.5 ± 1.4**
Free fatty acids (mM)	0.24 ± 0.03	0.21 ± 0.02
Triglycerides (mg/dl)	98 ± 148	144 ± 20
Cholesterol (mg/dl)	85 ± 5	115 ± 6**
Leptin (ng/ml)	19.4 ± 5.0	83.2 ± 18.7*

Data are mean ± SEM.; *$P < 0.05$ or **$P < 0.01$ vs. controls; n = 7-9/group by Students *t* test.